

# Gamma-ray lines from cosmic-ray interactions with interstellar dust grains

Vincent Tatischeff and Jürgen Kiener

*Centre de Spectrométrie Nucléaire et de Spectrométrie de Masse, IN2P3-CNRS  
and Université Paris-Sud, F-91405 Orsay Cedex, France*

---

## Abstract

As pointed out by Lingenfelter and Ramaty (1977), the shapes of some  $\gamma$ -ray lines produced by cosmic-ray interactions with the interstellar medium potentially contain valuable information on the physical properties of dust grains, including their compositions and size distributions. The most promising of such lines are at 847, 1369, 1779 and 6129 keV, from  $^{56}\text{Fe}^*$ ,  $^{24}\text{Mg}^*$ ,  $^{28}\text{Si}^*$  and  $^{16}\text{O}^*$ , respectively. We performed detailed calculations of their profiles using, in particular, available laboratory measurements combined with optical model calculations to evaluate the energy distributions of the recoiling excited nuclei. We show that the line shapes are mainly sensitive to relatively large interstellar grains, with radii  $\gtrsim 0.25 \mu\text{m}$ . Line fluxes from the inner Galaxy are then predicted.

*Key words:* cosmic rays, gamma rays: theory, dust

*PACS:* 98.70.Sa, 98.70.Rz, 98.38.Cp

---

## 1 Introduction

Observations of nuclear interaction  $\gamma$ -ray lines from the interstellar medium (ISM) would provide a unique tool to study Galactic cosmic-ray ions at non-relativistic energies, as well as the physical conditions of the emitting regions. If the lines produced in the gaseous phase are expected to be significantly Doppler-broadened, some lines produced in interstellar dust grains can be very narrow, because some of the excited nuclei can stop in solid materials before emitting  $\gamma$ -rays (Lingenfelter and Ramaty, 1977; Ramaty et al., 1979). The latter are prime candidates for detection with  $\gamma$ -ray telescopes having high spectral resolution, such as the *INTEGRAL* spectrometer (SPI).

An illustrative  $\gamma$ -ray spectrum is shown in figure (1). It was obtained in a recent experiment performed at Orsay (Kiener et al., in preparation), in which

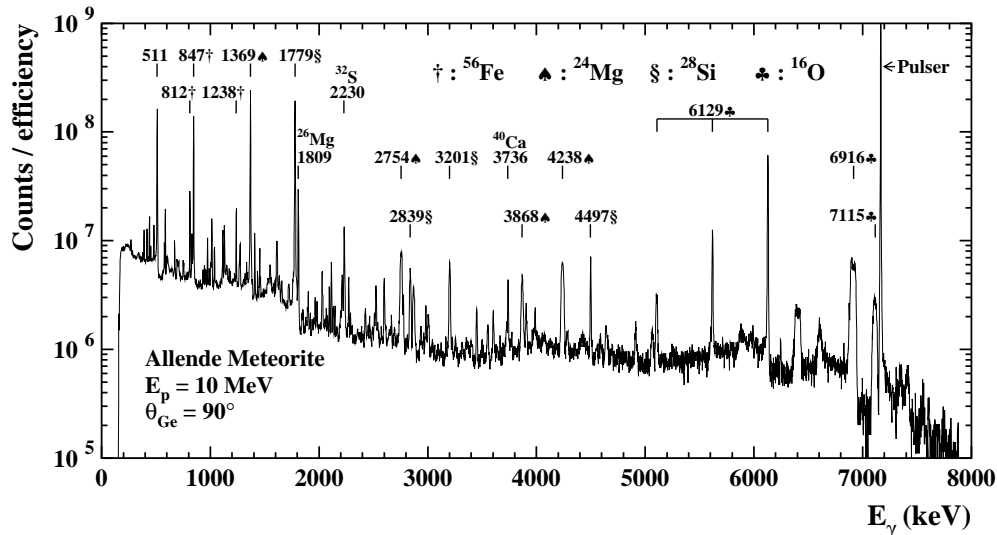


Fig. 1. Observed  $\gamma$ -ray spectrum from the bombardment of a thick sample of the Allende meteorite with 10-MeV protons. The most intense lines are labeled with their nominal energies and the target nuclei from which the  $\gamma$ -rays are produced. For the 6129-keV line, the single and double escape peaks are also indicated.

a thick sample of the Allende meteorite ( $\sim 5$  mm in diameter) was bombarded with 10-MeV protons. The Allende meteorite belongs to the class of carbonaceous chondrites and has a composition close to cosmic, except for the volatile elements. The strongest lines (apart from the 511-keV emission) originate from reactions with the most abundant isotopes:  $^{16}\text{O}$ ,  $^{24}\text{Mg}$ ,  $^{28}\text{Si}$  and  $^{56}\text{Fe}$ . One point of particular interest is that the  $^{16}\text{O}^*$  line at 6129 keV is much narrower than the two other  $^{16}\text{O}^*$  lines at 6916 and 7115 keV. This is because the 6.13-MeV state is relatively long-lived ( $T_{1/2}=18.4$  ps), such that the recoiling  $^{16}\text{O}^*$  nuclei can come to rest in the target before the 6.129-keV  $\gamma$ -ray is emitted, whereas the 6.92- and 7.12-MeV states ( $T_{1/2}=4.7$  and 8.3 fs, respectively) mostly de-excite in flight. The 6129-keV line, as well as the intense lines at 847 keV from  $^{56}\text{Fe}^*$  ( $T_{1/2}=6.1$  ps), 1369 keV from  $^{24}\text{Mg}^*$  ( $T_{1/2}=1.35$  ps) and 1779 keV from  $^{28}\text{Si}^*$  ( $T_{1/2}=475$  fs) are the prime candidates to scrutinize the interstellar dust grains through their  $\gamma$ -ray emission.

We have calculated in detail the shapes of these four lines as they are produced by cosmic-ray interactions with the ISM. The interaction model and the results are presented in sections (2) and (3), respectively. In section (4), we evaluate the intensities of the predicted emissions from the inner Galaxy.

## 2 Interaction model

To calculate the line profiles, we used a Monte-Carlo method similar to that described in Ramaty et al. (1979). Each event in the simulation corresponds

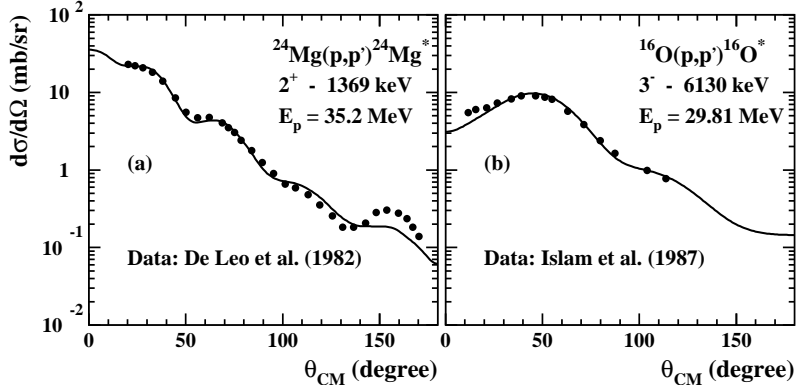


Fig. 2. Differential inelastic scattering cross sections for the reactions (a)  $^{24}\text{Mg}(p,p')^{24}\text{Mg}_{1369}^*$  at  $E_p=35.2$  MeV and (b)  $^{16}\text{O}(p,p')^{16}\text{O}_{6130}^*$  at  $E_p=29.81$  MeV. Solid curves – coupled-channel calculations.

to a  $\gamma$ -ray producing nuclear reaction of a cosmic-ray proton or  $\alpha$ -particle with a target nucleus either in the gas or locked up in a spherical and homogeneous dust grain of the ISM. The  $\gamma$ -rays can be produced by inelastic scattering reactions, e.g.  $^{16}\text{O}(p,p'\gamma_{6129})^{16}\text{O}$ , by  $(p,n)$  reactions followed by electron capture or positron emission, e.g.  $^{56}\text{Fe}(p,n)^{56}\text{Co}(\epsilon-\beta^+)^{56}\text{Fe}_{847}^*$  ( $T_{1/2}(^{56}\text{Co})=77.2$  d), or by spallation reactions, e.g.  $^{20}\text{Ne}(p,p\alpha\gamma_{6129})^{16}\text{O}$ . The total cross sections are from Kozlovsky et al. (2002), except for the reactions  $^{24}\text{Mg}(p,n)^{24}\text{Al}(\beta^+)^{24}\text{Mg}_{1369}^*$  ( $T_{1/2}(^{24}\text{Al})=2.053$  s) and  $^{28}\text{Si}(p,n)^{28}\text{P}(\beta^+)^{28}\text{Si}_{1779}^*$  ( $T_{1/2}(^{28}\text{P})=270.3$  ms). We estimated the contribution of the  $^{24}\text{Mg}(p,n)^{24}\text{Al}$  channel from the data of Kiang et al. (1989) and assumed the same relative contribution for the reaction  $^{28}\text{Si}(p,n)^{28}\text{P}$ .

The energy distribution of the recoiling excited nuclei were calculated from the differential cross sections. The latter were obtained from a large number of experimental data, completed with extensive coupled-channel calculations with the code ECIS94 (Raynal, 1994). Two examples of differential inelastic scattering cross sections are shown in figure (2).

The stopping powers of the nuclei recoiling in the grain material were calculated with the code TRIM (Ziegler, 1985). For these calculations, the grain composition was assumed to be  $(\text{MgSiFe})\text{O}_4$ , which is characteristic of interstellar silicates (e.g. Dwek et al., 1997).

To estimate the cosmic-ray proton interstellar spectrum, we used the disk-halo propagation model of Jones et al. (2001). Coulomb and ionization energy losses were taken from Mannheim and Schlickeiser (1994). For the proton inelastic cross sections, we used the empirical formula given in Moskalenko et al. (2002). Solar-modulated spectra, calculated from the force-field approximation, were fitted to measured proton fluxes (fig. 3). We found the best fit to be provided by the source spectrum  $\dot{Q}(p)dp \propto p^{-2.4}dp$ , where  $p$  is the proton momentum. For simplicity, we used the same form for the  $\alpha$ -particle LIS

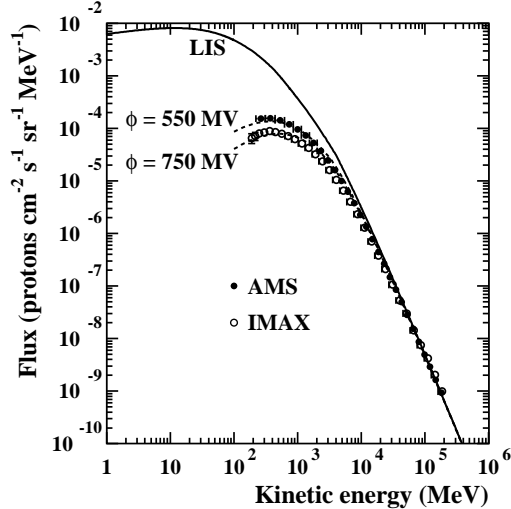


Fig. 3. Cosmic-ray proton local interstellar spectrum (LIS; solid curve) and solar-modulated spectra for two force-field potentials,  $\phi=550$  and  $750$  MV (dashed curves). AMS: Alcaraz et al. (2000); IMAX: Menn et al. (2000).

spectrum as for the protons, with an abundance ratio  $\alpha/p=0.1$ .

### 3 Gamma-ray line profiles

Calculated  $\gamma$ -ray line profiles are shown in figure (4) for different interstellar grain size distributions. We assumed that all the available refractory elements Mg, Si and Fe, and half of the O are locked up in silicate grains, whereas the volatile elements Ne and S (which contribute through spallation reactions to the 6129- and 1779-keV lines, respectively) are in the gaseous phase (see Savage and Sembach, 1996; Dwek et al., 1997). The dotted curves were obtained for the commonly used MRN (Mathis et al., 1977) size distribution: an  $a^{-3.5}$  power law in grain radii  $a$  from  $a_{min}=5$  nm (see Dwek et al., 1997) to  $a_{max}=0.25$   $\mu\text{m}$ . We see that there are little differences between these spectra and those calculated assuming that all the target nuclei are in the interstellar gas (thick, grey curves). In particular, the two profiles of the 6129-keV line are nearly identical, because almost all of the  $^{16}\text{O}$  nuclei excited within dust grains of radius  $<0.25$   $\mu\text{m}$  escape from the solids before decaying.

The dashed curves were calculated for the same power law distribution, but with  $a_{max}=2$   $\mu\text{m}$ . The extension of the grain radii beyond the MRN limit of  $0.25$   $\mu\text{m}$  is motivated by the observations with dust detectors aboard the *Ulysses* and *Galileo* spacecrafts of relatively large interstellar grains entering the solar system (Landgraf et al., 2000), as well as by models of scattering halos observed around X-ray sources (Witt et al., 2001). The thin, solid curves were obtained by further extending the MRN distribution to  $a_{max}=10$   $\mu\text{m}$ .

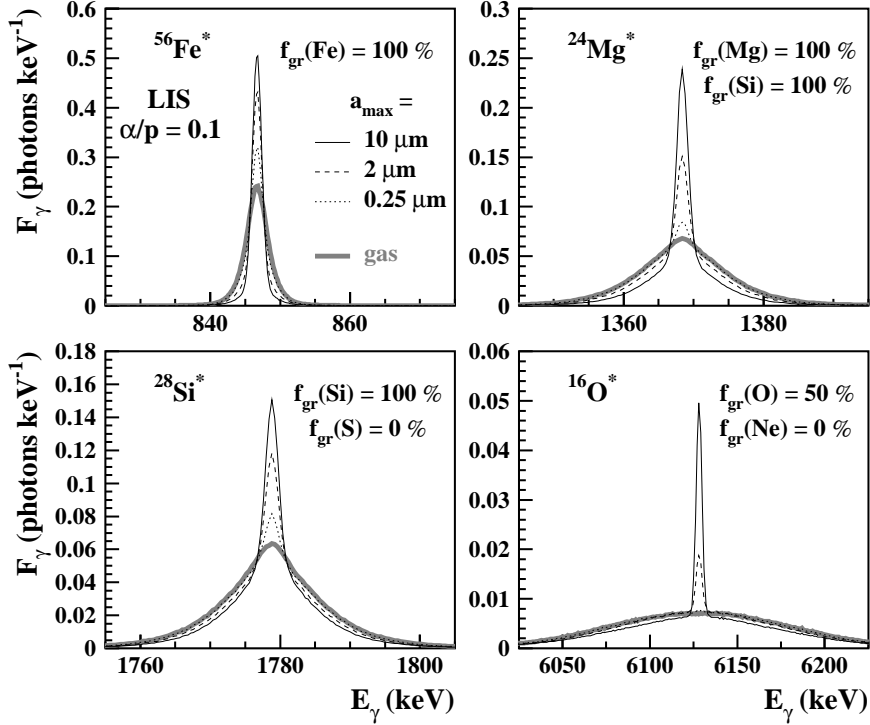


Fig. 4. Profiles of the  $\gamma$ -ray lines at 847 keV ( $^{56}\text{Fe}^*$ ), 1369 keV ( $^{24}\text{Mg}^*$ ), 1779 keV ( $^{28}\text{Si}^*$ ) and 6129 keV ( $^{16}\text{O}^*$ ), excited in cosmic-ray proton and  $\alpha$ -particle interactions with interstellar gas and dust grains. The calculated spectra are normalized to one photon emitted in each line and convolved with the SPI response function. Thin curves – grain size distributions following an  $a^{-3.5}$  power law in radii from  $a_{\min}=5$  nm to  $a_{\max}=0.25$   $\mu\text{m}$  (dotted curves), 2  $\mu\text{m}$  (dashed curves) and 10  $\mu\text{m}$  (solid curves). For each  $\gamma$ -ray line, the fractions of target nuclei assumed to be in the grains are indicated. Thick, grey curves – all target nuclei are assumed to be in the gas.

Such large grains are typical of presolar grains of stardust found in primitive meteorites (Zinner, 1998) and should exist in various circumstellar media. We see that for these two grain size distributions, the very narrow component of the  $^{24}\text{Mg}^*$ ,  $^{28}\text{Si}^*$  and  $^{16}\text{O}^*$  lines could in principle be resolved with SPI. The sensitivity of these line shapes to micrometer-sized particles provides a promising method for tracing large dust grains in the ISM.

#### 4 Gamma-ray line fluxes from the inner Galaxy

The  $\gamma$ -ray line intensities from the inner Galaxy were estimated by normalizing the emissivity calculations to the observed flux of high-energy  $\gamma$ -rays ( $>70$  MeV) due to  $\pi^0$  production and decay. We derived the latter from Büsching et al. (2001, fig. 1; EGRET data of observing phases 1-4):  $\Phi_{\gamma}^{\pi^0} \simeq 8.3 \times 10^{-5}$  photons  $\text{cm}^{-2}$   $\text{s}^{-1}$ , for  $-40^\circ < \ell < 40^\circ$  and  $-6^\circ < b < 6^\circ$ . We used

the model of Dermer (1986) to calculate the production of  $\pi^0$ -decay  $\gamma$ -rays by cosmic-rays with the LIS spectrum of figure (3). We assumed that the metal abundances in the inner Galaxy are on the average twice solar. We then obtained for the fluxes of the 847-, 1369-, 1779- and 6129-keV lines excited in proton and  $\alpha$ -particle interactions with both interstellar gas and dust grains:  $5.6 \times 10^{-8}$ ,  $7.5 \times 10^{-8}$ ,  $4.3 \times 10^{-8}$  and  $3.1 \times 10^{-7}$  photons  $\text{cm}^{-2} \text{s}^{-1}$ , respectively. In comparison, the calculated flux of the relatively strong line at 4438 keV from  $^{12}\text{C}^*$  (FWHM  $\simeq$  150 keV) is  $7.1 \times 10^{-7}$  photons  $\text{cm}^{-2} \text{s}^{-1}$  and that of the so-called  $\alpha$ - $\alpha$  line at  $\sim$ 450 keV (complex line shape with FWHM  $\simeq$  80 keV; see Tatischeff et al., 2001) is  $3.9 \times 10^{-7}$  photons  $\text{cm}^{-2} \text{s}^{-1}$ . All these diffuse emission fluxes are far below the SPI sensitivity, such that a near future detection of nuclear interaction  $\gamma$ -ray lines from the inner Galaxy is unlikely, unless there is a large population of Galactic cosmic-rays with kinetic energies below the threshold for  $\pi^0$  production (290 MeV for  $p$ +H collisions). Such a distinct cosmic-ray component predominant at low energies has been proposed to account for the quasi linear correlation between Be and Fe abundances for metallicities  $[\text{Fe}/\text{H}] < -1$  (e.g. Cassé et al., 1995).

## Acknowledgements

We acknowledge F. Boulanger for usefull discussions.

## References

- Alcaraz, J. et al., 2000. Phys. Lett. B490, 27.  
 Büsching, I., Pohl, M., Schlickeiser, R., 2001. A&A 377, 1056.  
 Cassé, M., Lehoucq, R., Vangioni-Flam, E., 1995. Nature 373, 318.  
 De Leo, R. et al., 1982. Phys. Rev. C25, 107.  
 Dermer, C.D., 1986. A&A 157, 223.  
 Dwek, E. et al., 1997. ApJ 475, 565.  
 Islam, M.S., Finlay, R.W., Petler, J.S., 1987. Nucl. Phys. A464, 395.  
 Jones, F.C., Lukasiak, A., Ptuskin, V., Webber, W., 2001. ApJ 547, 264.  
 Kiang, G.C. et al., 1989. Nucl. Phys. A499, 339.  
 Kozlovsky, B., Murphy, R.J., Ramaty, R., 2002. ApJS 141, 523.  
 Landgraf, M., Baggaley, W.J., Grn, E., Krger, H., Linkert, G., 2000. J. Geophys. Res. 105, 10343.  
 Lingenfelter, R.E., Ramaty, R., 1977. ApJ 211, L19.  
 Mannheim, K., Schlickeiser, R., 1994. A&A 286, 983.  
 Mathis, J.S., Rumpl, W., Nordsieck, K.H., 1977. ApJ 217, 425.  
 Menn, W. et al., 2000. ApJ 533, 281.

- Moskalenko, I.V., Strong, A.W., Ormes, J.F., Potgieter, M.S., 2002. *ApJ* 565, 280.
- Ramaty, R., Kozlovsky, B., Lingenfelter, R.E., 1979. *ApJS* 40, 487.
- Raynal, J., 1994. Notes on Ecis94, Note CEA-N-272 (unpublished).
- Savage, B.D., Sembach, K.R., 1996. *ARA&A* 34, 279.
- Tatischeff, V., Thibaud, J.-P., Kiener, J., Cassé, M., Vangioni-Flam, E., 2001. Proc. of the 4th INTEGRAL Workshop, Exploring the Gamma-Ray Universe, ESA Publication SP-459, p. 105.
- Witt, A.N., Smith, R.K., Dwek, E., 2001. *ApJ* 550, L201.
- Ziegler, J.F., 1985. *The Stopping and Range of Ions in Solids* (Pergamon Press, New York, 1985). See also URL <http://www.SRIM.org/>
- Zinner, E., 1998. *Annu. Rev. Earth Planet. Sci.* 26, 147.